ARMY RESEARCH LABORATORY

The Influence of Ply Waviness With Nonlinear Shear on the Stiffness and Strength Reduction of Composite Laminates

Travis A. Bogetti
U.S. ARMY RESEARCH LABORATORY

John W. Gillespie, Jr.
CENTER FOR COMPOSITE MATERIALS

Mark A. Lamontia
E.I. DU PONT NEMOURS & CO., INC.

ARL-TR-585 October 1994

NOTICES

Destroy this report when it is no longer needed. DO NOT return it to the originator.

Secondary distribution of this report is prohibited.

The findings of this report are not to be construed as an official Department of the Army position, unless so designated by other authorized documents.

The use of trade names or manufacturers' names in this report does not constitute indorsement of any commercial products.

REPORT DOCUMENTATION PAGE

Form Approved
OMB No. 0704-0188

1. AGENCY USE ONLY (Leave blank)	2. REPORT DATE	3. REPORT TYPE AND DATES COVERED
	October 1994	Final, May 1992–Apr 1993

4. TITLE AND SUBTITLE

The Influence of Ply Waviness With Nonlinear Shear on the Stiffness and Strength Reduction of Composite Laminates

5. FUNDING NUMBERS

PR: 1L162618AH80

6. AUTHOR(S)

Travis A. Bogetti, John W. Gillespie, Jr.,[a] and Mark A. Lamontia[b]

7. PERFORMING ORGANIZATION NAME(S) AND ADDRESS(ES)

U.S. Army Research Laboratory
ATTN: AMSRL-WT-PD
Aberdeen Proving Ground, MD 21005-5066

8. PERFORMING ORGANIZATION REPORT NUMBER

9. SPONSORING/MONITORING AGENCY NAME(S) AND ADDRESS(ES)

U.S. Army Research Laboratory
ATTN: AMSRL-OP-AP-L
Aberdeen Proving Ground, MD 21005-5066

10. SPONSORING/MONITORING AGENCY REPORT NUMBER

ARL-TR-585

11. SUPPLEMENTARY NOTES

[a]John W. Gillespie, Jr. is employed by the Center for Composite Materials.
[b]Mark A. Lamontia is employed by E.I. Du Pont Nemours & Co., Inc.

12a. DISTRIBUTION/AVAILABILITY STATEMENT

Approved for public release; distribution is unlimited.

12b. DISTRIBUTION CODE

13. ABSTRACT (Maximum 200 words)

The influence of ply waviness with nonlinear shear material response on the mechanical performance of composite laminates is studied. An analytic model, based on a three-dimensional laminated media analysis, is developed to predict the effective nonlinear laminate behavior associated with ply waviness. An undulating [0] ply in a [90/0/90] sublaminate configuration and an undulating [±β] ply in a [90/±β/90] sublaminate configuration are two types of ply waviness considered. An incremental loading strategy is employed wherein piecewise linear solutions are superimposed to obtain the overall nonlinear stress/strain response of composite laminates with wavy plies. The analysis also predicts individual ply stress and strain distributions within the wavy ply configuration. The maximum stress failure criteria is used to predict ply failure in local regions within the wavy ply configuration, and a progressive failure methodology is adopted to permit local load redistribution. Results are presented which offer fundamental insight into the dominant mechanisms for stiffness and strength reduction in composite laminates exhibiting ply waviness and nonlinear shear material behavior.

14. SUBJECT TERMS

composite materials, ply waviness, nonlinear shear, stiffness, strength

15. NUMBER OF PAGES

27

16. PRICE CODE

17. SECURITY CLASSIFICATION OF REPORT	18. SECURITY CLASSIFICATION OF THIS PAGE	19. SECURITY CLASSIFICATION OF ABSTRACT	20. LIMITATION OF ABSTRACT
UNCLASSIFIED	UNCLASSIFIED	UNCLASSIFIED	UL

INTENTIONALLY LEFT BLANK.

ACKNOWLEDGMENT

This work was sponsored by the Defense Advanced Research Projects Agency (DARPA), Naval Technology Program, under contract No. MDA972-89-C-0043.

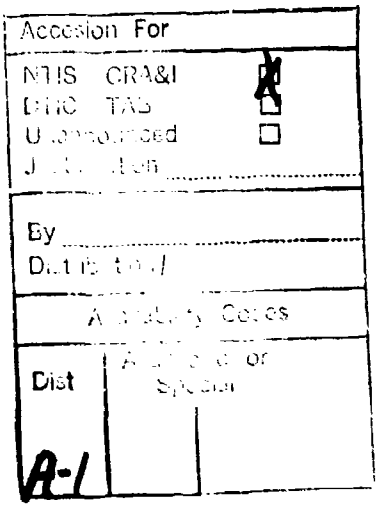

INTENTIONALLY LEFT BLANK.

TABLE OF CONTENTS

INTENTIONALLY LEFT BLANK.

LIST OF FIGURES

LIST OF TABLES

INTENTIONALLY LEFT BLANK.

1. INTRODUCTION

1.1 Background. Ply waviness, a manufacturing-induced anomaly in composite materials, is a subject that has received considerable attention from the composites community (Adams and Hyer 1992; Bogetti et al. 1991a, 1991b; Garala 1989; Highsmith et al. 1992; Hyer et al. 1988; Jortner 1984; Telgadas and Hyer 1990). Ply waviness has been demonstrated experimentally, numerically, and analytically to significantly reduce the mechanical performance of composite laminates and structures. Hyer et al. (1988) and Telgadas and Hyer (1990) have combined analytic and numerical models to study ply waviness in laminated composite cylinders for hydrostatic pressure load-bearing applications. Adams and Hyer (1992) and Garala (1989) have experimentally demonstrated the deleterious effects ply waviness can have on the mechanical performance of composite laminates and structures. Bogetti et al. (1991a, 1991b) have developed linear-elastic analytic models to study the influence of ply waviness on stiffness and strength reduction in composite laminates. The importance of shear material nonlinearity in wavy ply analyses has also been recognized (Adams and Hyer 1992). In addition, interlaminar shear has been identified as at least one dominant failure mechanism associated with ply waviness (Bogetti et al. 1991a, 1991b; Hyer et al. 1988; Telgadas and Hyer 1990).

1.2 Problem Statement. In this work, analytic models are developed to predict the effective three-dimensional nonlinear stress/strain mechanical behavior of two different types of wavy ply geometries. These models can be used to quantify the synergistic effects ply waviness can have on the mechanical performance of composite laminates and filament-wound structures.

The two wavy ply geometries under investigation include a [90/0/90] configuration and a [90/±β/90] configuration. A schematic illustrating ply waviness in the [90/0/90] configuration is shown in Figure 1a, where an undulating [0] ply is embedded in [90] plies having straight fibers. A typical [±β] configuration is presented in Figure 1b to illustrate the nature of the ply undulation at a tow or yarn crossover region in a filament-wound structure. In the full [90/±β/90] configuration (shown later), the [±β] plies will be embedded between two [90] plies. Both of these wavy ply geometries represent sublaminate configurations which are commonly employed in filament-wound structures. The models developed in this work portray realistic ply-level microstructural anomalies (waviness) characteristic of the filament winding process.

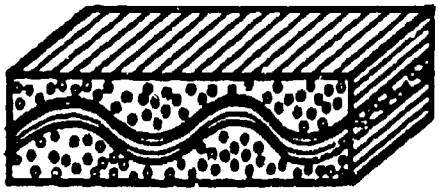

(a) [90/0/90] Model

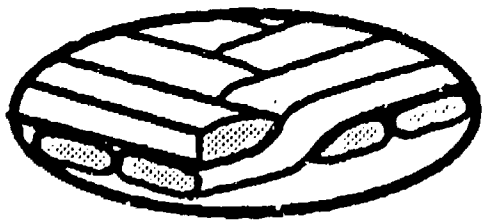

(b) [±β] Model

Figure 1. Wavy ply geometries.

2. ANALYSIS

2.1 Geometry Definitions for the [90/0/90] Model. From the wavy ply configuration depicted in Figure 1a, a unit cell is first idealized (see Figure 2a). A half-sine wave segment of the undulation is selected as a representative element. Ply waviness is assumed to exist in the x-direction only. The length of the unit cell is L, the total thickness is h_t, and the amplitude of the undulation is A. The unit cell consists of an undulating [0] ply (ply 2), with thickness h_f lying between two [90] ply regions (plies 1 and 3). The [90] plies are aligned in the y-direction and are assumed to have no undulation.

Detailed mathematical descriptions of the individual ply surfaces within the unit cell, expressed as a function of x, are required. Referring to Figure 2a, the following equations are used to define the ply surface distances from the laminate midplane along the half-sine wave shaped undulation, where the first subscript denotes the ply number and the second subscript (t or b) denotes the top or bottom ply surface, respectively.

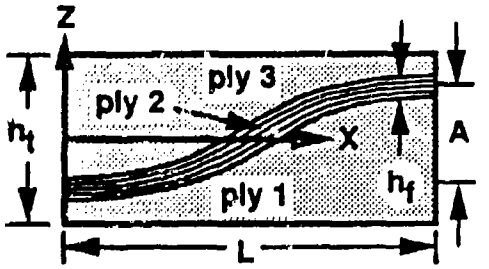

(a) [90/0/90] Unit Cell

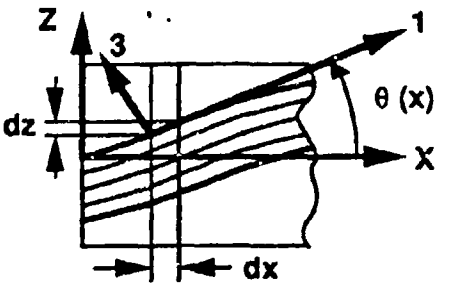

(b) Out-of-Plane Orientation Angle Definition

Figure 2. Unit cell descriptions.

$$h_{1b}(x) = -h_t/2$$

$$h_{1t}(x) = h_{2b}(x) = -A/2 - h_f/2 + \left[1 + \sin\left(\frac{\pi}{L}\left(x - \frac{L}{2}\right)\right)\right] A/2$$

$$h_{2t}(x) = h_{3b}(x) = -A/2 + h_f/2 + \left[1 + \sin\left(\frac{\pi}{L}\left(x - \frac{L}{2}\right)\right)\right] A/2$$

$$h_{3t}(x) = h_t/2, \qquad (1)$$

A local out-of-plane undulation angle, θ, is also needed. This local angle changes along the undulation (i.e., is a function of x), but is assumed constant within any one "incremental" segment. Referring to Figure 2b, θ can be defined as a function of x as

$$\theta(x) = \tan^{-1}\left[\frac{dz}{dx}\right], \qquad (2)$$

where dx is the width of an incremental segment along the unit cell undulation in the x-direction and dz is the corresponding incremental change in ply surface height.

2.2 Geometry Definitions for the [90/±β/90] Model. The unit cell idealization of the crossover region (including the [90] plies) is shown in Figures 3a and 3b. Geometric parameters of the unit cell are quantified by the winding angle, β, defined with respect to the x-direction, the amplitude of the ply (tow or yarn) undulation (assumed to be equal to h_f), the total sublaminate thickness, h_t, and the unit cell length, L, of the sinusoidal crossover region. An out-of-plane rotation angle, θ, at the crossover region

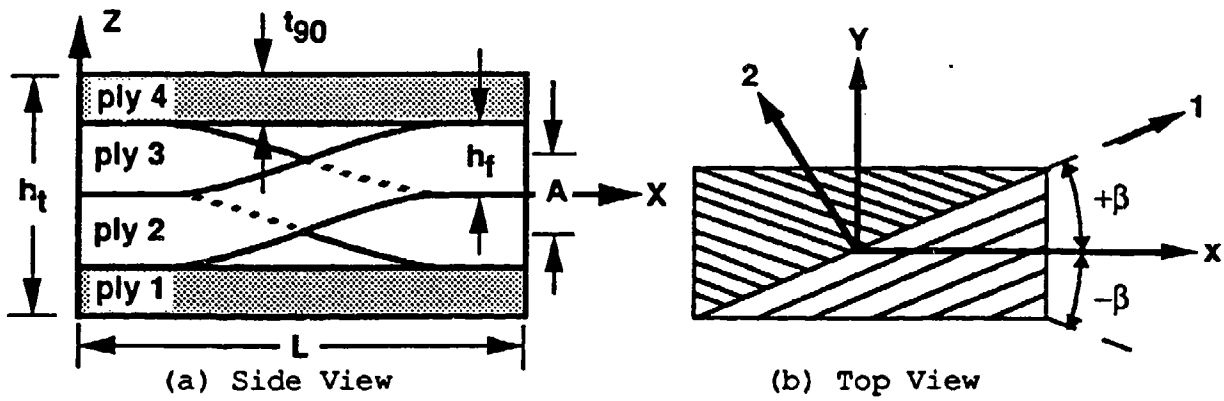

Figure 3. [90/±β/90] unit cell.

is assumed to exist only in the [±β] plies. The [±β] plies are embedded between two [90] plies of equal and constant thickness (t_{90}) which are assumed to have no undulation.

Descriptions of the individual ply surfaces within the unit cell, expressed as a function of x, are also required. Referring to Figure 3a, the following distances from the laminate midplane to the ply surfaces along the half-sine wave-shaped undulations are defined

$$
\begin{aligned}
h_{1t}(x) &= -h_f \\
h_{1b}(x) &= -(h_f + t_{90}) \\
h_{2t}(x) &= \left[1 + \sin\left(\frac{\pi}{L}\left(x - \frac{L}{2}\right)\right)\right] h_f/2 \\
h_{2b}(x) &= -h_f + \left[1 + \sin\left(\frac{\pi}{L}\left(x - \frac{L}{2}\right)\right)\right] h_f/2 \\
h_{3t}(x) &= h_f - \left[1 + \sin\left(\frac{\pi}{L}\left(x - \frac{L}{2}\right)\right)\right] h_f/2 \\
h_{3b}(x) &= -\left[1 + \sin\left(\frac{\pi}{L}\left(x - \frac{L}{2}\right)\right)\right] h_f/2 \\
h_{4b}(x) &= h_f \\
h_{4t}(x) &= (h_f + t_{90}).
\end{aligned}
\tag{3}
$$

The local out-of-plane undulation angle, θ, for each of the [$\pm\beta$] plies is defined analogous to the [0] ply in the [90/0/90] model presented in Figure 2b.

2.3 Laminate Analogy. The analysis presented below is generic in that it can be applied to each of the two types of wavy ply geometries described above. The effective nonlinear mechanical behavior of the unit cell is assumed to be representative of the response of the entire wavy ply configuration. The unit cell is first divided into discrete incremental segments of equal width, dx, in the direction of undulation (the x-direction). A systematic laminated media analogy is then applied to each individual segment before the effective response of the entire unit cell is formulated.

An effective stress/strain constitutive relationship for each discrete segment within the unit cell is first computed according to a three-dimensional laminated media analysis (Chou et al. 1972)

$$\overline{\sigma}_i = \overline{C}_{ij}\,\overline{\varepsilon}_j \quad \text{for} \quad (i, j = 1, 2, 3, 4, 5, 6). \tag{4}$$

The effective $\overline{C}_{ij}$ stiffness matrices in Equation 4 are defined according to the following relations

$$\overline{C}_{ij} = \sum_{k=1}^{n} V^k \left[C_{ij}^k - \frac{C_{13}^k\, C_{3j}^k}{C_{33}^k} + \frac{C_{i3}^k \sum_{l=1}^{n} \dfrac{V^l\, C_{3j}^l}{C_{33}^l}}{C_{33}^k \sum_{l=1}^{n} \dfrac{V^l}{C_{33}^l}} \right] \quad \text{for} \quad (i, j = 1, 2, 3, 6), \tag{5}$$

$$\overline{C}_{ij} = \overline{C}_{ji} = 0 \quad \text{for} \quad (i = 1, 2, 3, 6;\ j = 4, 5) \tag{6}$$

and

$$\overline{C}_{ij} = \left[\frac{\sum_{k=1}^{n} \dfrac{V^k}{\Delta_k} C_{ij}^k}{\sum_{k=1}^{n} \sum_{l=1}^{n} \dfrac{V^k V^l}{\Delta_k \Delta_l} \left(C_{44}^k\, C_{55}^l - C_{45}^k\, C_{54}^l \right)} \right] \quad \text{for} \quad (i, j = 4, 5), \tag{7}$$

where

$$\Delta_k = \begin{vmatrix} C_{44}^k & C_{45}^k \\ C_{54}^k & C_{55}^k \end{vmatrix} = C_{44}^k \; C_{55}^k - C_{45}^k \; C_{54}^k \,, \tag{8}$$

and n is the total number of plies in the segment, V^k is the ratio of the thickness of the k^{th} ply to the total unit cell thickness (i.e., $(h_{k+1} - h_k)/h_t$), and C_{ij}^k is the lamina stiffness matrix for the k^{th} ply in the segment, which is defined in the global laminate (x-y-z) coordinate system and therefore accounts for any rotations (in-plane and/or out-of-plane) due to ply waviness. Tensoral rotations are used to compute the C_{ij}^k's from the typical engineering constants of the straight lamina (i.e., E_1, E_2, E_3, ν_{12}, ν_{13}, ν_{23}, G_{12}, G_{13}, and G_{23}) and corresponding rotation angles between the global laminate (x-y-z) and principal material (1-2-3) coordinate systems (Lehknitski 1963).

The local h_i values of the plies (within each segment) are defined by Equation 1 for the [90/0/90] model and Equation 3 for the [90/±β/90] model. The C_{ij}^k's for the [90] plies (in both models) are constant along the x-direction. The C_{ij}^k's for the [0] and [±β] plies, however, must take into account the out-of-plane (θ(x)) orientations which vary along the unit cell. For example, segments in the [90/0/90] model are represented by a three-ply laminate having out-of-plane rotations (θ(x)) in the C_{ij}^k matrices for the [0] ply, $C_{ij}^2(x)$. Segments in the [90/±β/90] model are represented by a four-ply laminate having both in-plane (±β) rotations and out-of-plane (θ(x)) rotations in the C_{ij}^k matrices for the (±β) plies, $C_{ij}^2(x)$, and $C_{ij}^3(x)$. Compliance matrices, $\bar{s}_{ij}$, for each dx segment within the unit cell are then computed through matrix inversion of the segment stiffness matrices, $\bar{C}_{ij}$.

2.4 Nonlinear Lamina Constitutive Relations. Material nonlinearity is introduced in the principal shear directions of the lamina constitutive relations, 23, 13, and 12. All other mechanical properties are assumed constant. The Ramberg-Osgood Equation is adopted here to represent material nonlinearity (Richard and Blackloak 1969). The three-parameter equation relating stress explicitly as a continuous function of strain is given by

$$\tau(\gamma) = \frac{G^o \cdot \gamma}{(1 + (G^o \cdot \gamma/\tau^o)\, p)^{1/p}}, \tag{9}$$

where G^o is the initial linear shear modulus, τ^o is an asymptotic shear stress value, and p is a shape parameter.

Taking the derivative of Equation 9 with respect to strain yields an expression for the tangent modulus, G_t, as a continuous function of strain

$$G_t(\gamma) = \frac{d\tau}{d\gamma} = \frac{G^o \cdot \gamma}{(1 + (G^o \cdot \gamma/\tau^o)\ p)^{1+1/p}}. \tag{10}$$

Equation 10 is a convenient expression for determining the tangent or instantaneous shear moduli of the lamina within the wavy ply configuration. By continuously monitoring the principal shear strain level of each ply within each segment during incremental loading, the instantaneous moduli can be computed straightforwardly.

2.5 Incremental Formulation. The theoretical basis for the nonlinear incremental formulation is the "linear" analysis outlined above. The approach is to incrementally apply loads (defined in terms of average three-dimensional stresses) to the unit cell until the desired load level is reached. The Full Newton-Raphson Method is the incremental solution technique adopted in the analysis (Bathe and Cimento 1980). Solution convergence is based on a force tolerance criteria.

At the beginning of each load step, the instantaneous lamina properties for all plies in each segment of the unit cell are computed according to Equation 10. All other lamina properties are assumed constant. The instantaneous shear properties computed from Equation 10 are based on the current principal ply strain levels at the beginning of the load step. The instantaneous shear moduli will vary from ply to ply within a given segment and will also vary from segment to segment along the unit cell, depending on the local strain distributions. Once the tangent shear moduli are determined, the instantaneous compliance matrix, $\overline{s}_{ij}$, for each of the segments within the unit cell are computed, as outlined above. The effective incremental strains for each individual segment, due to an applied load increment, $\Delta\overline{\sigma}_j$, are computed according to

$$\Delta\overline{\varepsilon}_i^k = \overline{s}_{ij}^k\ \Delta\overline{\sigma}_j, \tag{11}$$

where the superscript k is used here as an index to denote the segment number. Note that the superscript k is not used on the load increment $\Delta\overline{\sigma}_j$, since it is assumed constant for all the segments within the unit cell. For each applied load increment, the effective strain increment for the entire unit cell is computed as the sum of all the segment strains by

$$\Delta\,\overline{\varepsilon}_i = \sum_{k=1}^{m} \Delta\overline{\varepsilon}_i^k, \tag{12}$$

where m denotes the total number of segments in the unit cell.

The incremental strategy used calls for the application of equal and successive load increments, $\Delta\overline{\sigma}_j$, to the unit cell and a continuous monitoring of the resulting strain increments within the unit cell. For each load step that is applied to the unit cell, a piecewise linear increment in unit cell strain is computed according to Equations 11 and 12. The nonlinear behavior of the wavy configuration is represented by an effective (average) stress-strain curve generated from the unit cell response to incremental loading. The total average stress at any point during the incremental loading is defined as the cumulative sum of all prior load increments applied to the unit cell. Mathematically, the total average stress acting on the unit cell, $\Delta\overline{\sigma}_j^T$ (for example, after nls load steps), is given by

$$\overline{\sigma}_j^T = \sum_{k=1}^{nls} \Delta\overline{\sigma}_j^k, \tag{13}$$

where the superscript k is used here as an index to denote the load increment. The corresponding total effective unit cell strain, $\overline{\varepsilon}_i^T$, is defined as the cumulative sum of all prior unit cell strain increments up to the current load level. For example, after nls load increments, the total unit cell strain is defined by

$$\overline{\varepsilon}_j^T = \sum_{k=1}^{nls} \Delta\overline{\varepsilon}_j^k. \tag{14}$$

The effective stress/strain behavior of the unit cell is therefore defined by the relationship generated between $\overline{\sigma}_j^T$ and $\overline{\varepsilon}_i^T$ over the prescribed load path history.

2.6 Failure Criteria. The maximum stress failure criteria is employed in the analysis. During the incremental loading, the total principal stress levels within each ply of each segment are calculated. When the principal stress level in a ply reaches the value of its corresponding allowable, as defined in the maximum stress failure criteria, the modulus associated with that ply and failure mode is set arbitrarily small for subsequent calculations. Accordingly, the ply retains its current stress level, but is prevented from carrying additional stress during subsequent incremental loading.

3. RESULTS

3.1 Input Summary. Wavy model input parameters required in the analysis include the material properties of the composite, the unit cell geometric parameters, and details of the incremental load strategy. An AS4/PEKK graphite/thermoplastic composite material system is used to illustrate the findings. Material properties and strength allowables for AS4/PEKK are listed in Tables 1 and 2, respectively. The Ramberg-Osgood parameters used to represent the nonlinear shear response of the AS4/PEKK system in the 23, 13, and 12 principal shear directions are summarized in Table 3. The corresponding shear stress/strain curves are presented in Figure 4. For this analysis, the asymptotic stress values are assumed to be equal to their corresponding ultimate strength allowables.

Table 1. Material Properties for AS4 Graphite/PEKK

E_1	(MPa)	1.17×10^5
E_2	(MPa)	9.66×10^3
E_3	(MPa)	9.66×10^3
ν_{12}		0.36
ν_{13}		0.36
ν_{23}		0.36

The incremental strategy requires one to define a load step size, $\Delta\overline{\sigma}_j$, and the total number of load increments to be applied. As with most incremental numerical techniques, solution accuracy is improved by decreasing the load step size. It is noted that convergence studies were conducted for all the examples presented in this work to ensure accurate numerical results.

Table 2. Strength Allowables for AS4 Graphite/PEKK

X1T	(MPa)	1.97×10^3
X2T	(MPa)	3.59×10^1
X3T	(MPa)	3.59×10^1
X1C	(MPa)	1.07×10^3
X2C	(MPa)	1.83×10^2
X3C	(MPa)	1.83×10^2
S12	(MPa)	1.31×10^2
S13	(MPa)	7.59×10^1
S23	(MPa)	3.79×10^1

Table 3. Ramberg-Osgood Shear Parameters for AS4/PEKK

G^0_{12}	(MPa)	6.76×10^3
G^0_{13}	(MPa)	6.76×10^3
G^0_{23}	(MPa)	4.34×10^3
τ^0_{12}	(MPa)	1.31×10^2
τ^0_{13}	(MPa)	7.59×10^1
τ^0_{23}	(MPa)	3.79×10
P_{12}		2.0
P_{13}		2.0
P_{23}		2.0

3.2 [90/0/90] Model Predictions. The first case study employs the [90/0/90] wavy model with the following geometric parameters; L = 0.127 cm, h_f = 0.0127 cm, h_i = 0.0381 cm, and A = 0.0127 cm. The unit cell configuration is incrementally loaded in uniaxial compression in the x-direction until ultimate failure. The following sections discuss the findings of this case study.

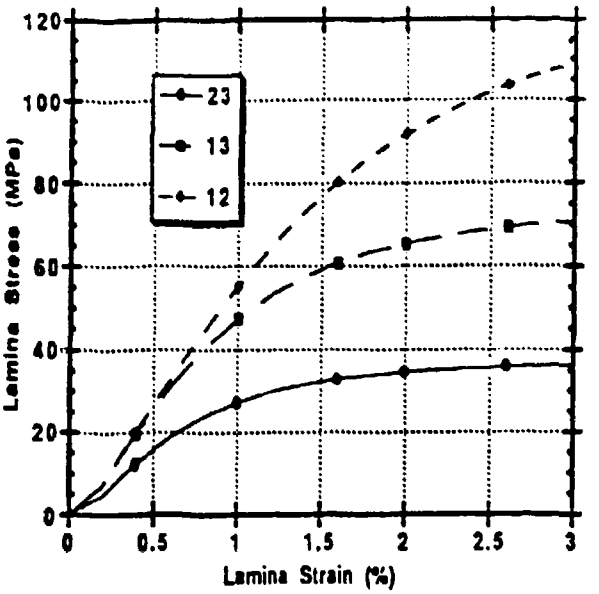

Figure 4. Nonlinear lamina shear stress/strain response for AS4/PEKK.

3.2.1 Comparison With Linear Analysis Predictions. The effective x-direction unit cell stress/strain response is first examined. A linear-elastic version of this example was conducted to provide a baseline for comparison with the nonlinear predictions. The shear moduli employed in the linear case are the Ramberg-Osgood initial shear moduli (see Table 3). The linear and nonlinear x-direction stress/strain response predictions of the unit cell are presented in Figure 5. Failure in the linear case is reached when any principal ply stress component, in any segment, reaches its corresponding strength allowable (see Table 2). Failure in the nonlinear case is reached when the unit cell can no longer sustain additional incremental loading (load divergence is detected). As expected, the stress/strain responses are similar at low levels of strain and diverge at higher strain levels, where nonlinear material softening occurs. The ultimate load levels are markedly different (195 MPa and 312 MPa for the linear and nonlinear cases, respectively). The failure mechanism in the linear case is interlaminar shear stress failure, σ_{13}, which occurs in the segment of the wavy configuration with the greatest ply undulation (maximum shear stress). In the nonlinear analysis, the interlaminar shear ply stress, σ_{13}, does not reach its ultimate but rather approaches it asymptotically. Consequently, the wavy configuration is permitted to bear load well beyond the load level predicted to cause failure in the linear analysis. As the additional load is applied, the nonlinearity of the strain response increases, to a point where divergence is detected (312 MPa). The following sections help to identify the fundamental mechanisms contributing to the overall nonlinear response of the wavy unit cell configuration.

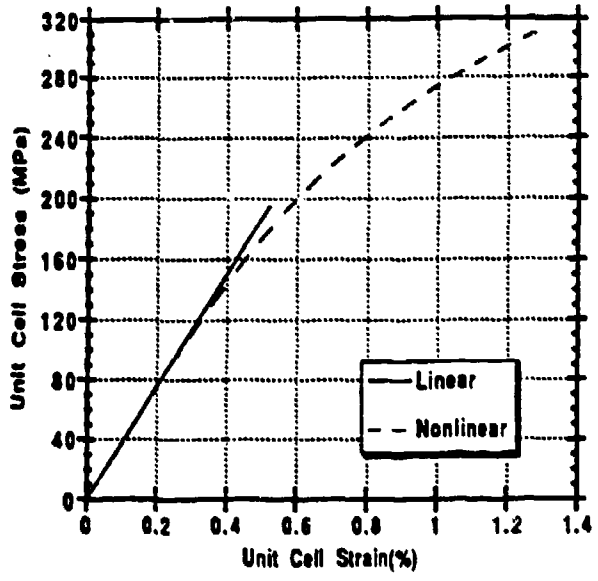

Figure 5. Nonlinear stress/strain response of the [90/0/90] model under uniaxial compression.

3.2.2 Development of Segment Strain Distributions. Under the constant average stress assumption, the segment strains which develop during incremental loading are expected to vary along the unit cell, peaking where the local out-of-plane [0] ply undulation angle is a maximum, at x = L /2. The development of nonlinear segment strain distributions within the unit cell is demonstrated in Figure 6 at load levels between 69 MPa and 276 MPa. Note that the large strains (nonlinear) begin to develop in segments with greater ply undulation and that they become increasingly more nonlinear with increasing load. This increased nonlinear behavior is due to the fact that as the interlaminar shear strains increase, the corresponding tangent moduli decrease and reduce the local compliance matrices within the segments.

3.2.3 Influence of Undulation Amplitude on the Nonlinear Response. The influence of undulation amplitude on the nonlinear x-direction stress/strain response of the [90/0/90] model (with the same geometric parameters and under the same loading condition as described above) was also examined. In Figure 7, the x-direction stress/strain responses of wavy unit cell configurations with undulation amplitudes A = 0.00000 cm, 0.00635 cm, and 0.01270 cm are presented. Note that the case for A = 0.00000 cm is linear to failure and is identical to what would be predicted by classical laminate analysis (524.8 MPa). This is the expected result since there are no undulation or nonlinear effects in this case. Comparing the

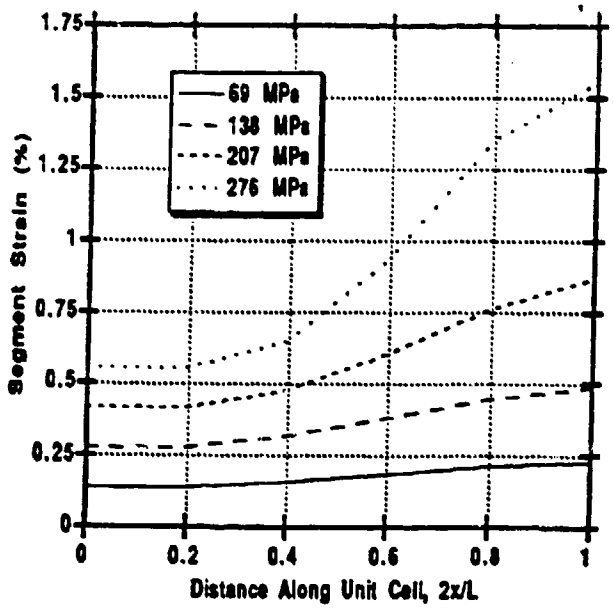

Figure 6. Development of segment strains within the [90/0/90] model under uniaxial compression.

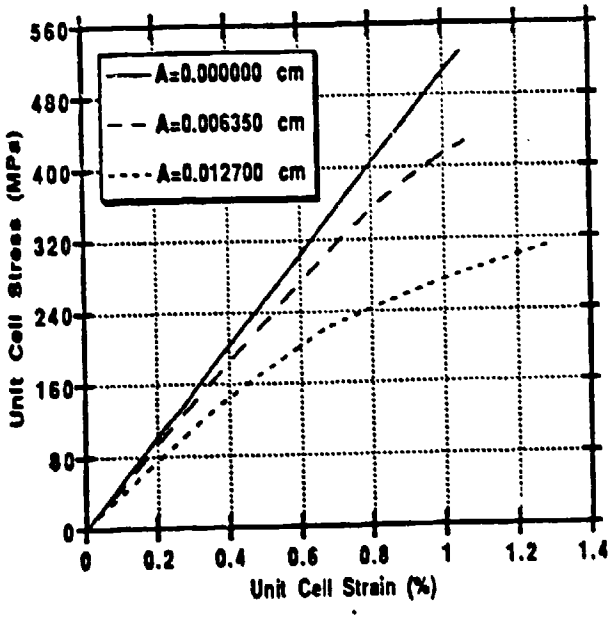

Figure 7. Influence of undulation amplitude on the nonlinear response of the [90/0/90] model under uniaxial compression.

other cases, it is shown that the ultimate unit cell strength decreases significantly with increasing undulation amplitude. It is noted, however, that these ultimate strengths are significantly higher than those predicted by the linear wavy analysis because of the previously discussed reasons (Figure 5).

3.3 [90/±β/90] Crossover Model Predictions. In our second case study, we present a comparison of the nonlinear and linear analysis predictions for the [90/±β/90] crossover model. In Figure 8, the nonlinear and linear stress/strain responses of the [90/±β/90] crossover model for β = 64°, 49°, and 20° are presented. The linear and nonlinear predictions of the initial moduli for the respective models are in good agreement. This is expected since at low load levels, linear material behavior is dominant. As with the [90/0/90] wavy model, the nonlinear analysis predicts significantly higher ultimate strength values than those of the linear analysis. Again, this is due to the fact that the dominant failure mechanism of the linear analysis, interlaminar shear failure, does not constitute catostrophic failure in the nonlinear analysis. It is noted that these [90/±β/90] crossover configurations exhibit substantially more nonlinearity than the [90/0/90] wavy configuration. This is due to the fact that the in-plane shear loading of the [±β] plies contribute an additional source of nonlinearity.

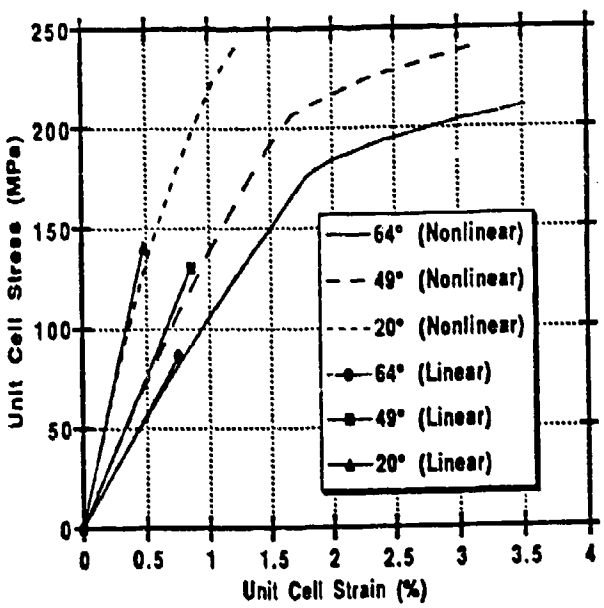

Figure 8. Nonlinear stress/strain response of the [90/±β/90] cross-over model under uniaxial compression.

4. CONCLUSIONS

An analytic model, based on a three-dimensional laminated media analysis, was developed to predict the effective nonlinear laminate behavior associated with ply waviness. An undulating [0] ply in a [90/0/90] sublaminate configuration and an undulating [±β] ply in a [90/±β/90] sublaminate configuration were two types of ply waviness considered. An incremental loading strategy was employed wherein piecewise linear solutions were superimposed to obtain the overall nonlinear stress/strain response of composite laminates with wavy plies.

The influence of ply waviness with nonlinear shear material response on the mechanical performance of composite laminates was studied. The nonlinear analysis revealed significant nonlinearity in the stress/strain response of both the wavy ply and crossover region configurations investigated. This nonlinear response was largely due to severe nonlinear straining in regions of the configuration where ply undulation was greatest. This is brought about by the decreasing tangent shear moduli associated with high shear straining within undulating plies. Strain distributions with the wavy ply configuration showed that segment strains in regions of the configuration with large ply undulations strained significantly more than segments with no undulation, which exhibited the usual linear response. At low load levels, the nonlinear and linear overall stress/strain responses for both the wavy ply and crossover configurations were similar. The most significant finding of the nonlinear analysis was that nonlinear ultimate strength predictions for the wavy ply and crossover configurations were significantly higher than linear predictions. Interlaminar shear is the dominant failure mechanism in the linear analysis strength predictions. In the nonlinear analysis, this failure mechanism does not constitute ultimate failure. Loading is permitted to continue as loads are redistributed to adjacent plies. This redistribution of load results in ultimate strength predictions for the nonlinear analysis as much as twice that predicted in the linear analysis. The models developed in this work portray realistic ply-level microstructural waviness characteristic of the filament winding process and therefore can be used to quantify the synergistic effects ply waviness can have on the mechanical performance of filament-wound structures.

INTENTIONALLY LEFT BLANK.

5. REFERENCES

Adams, D. O., and M. W Hyer. "Effects of Layer Waviness on Compression-Loaded Thermoplastic Composite Laminates." Technical Report, CCMS-92-06/VPI-E-92-06, Center for Composite Materials and Structures, Virginia Polytechic Institute, Blacksburg, VA, 1992.

Bathe, K. J., and A. P. Cimento. "Some Practical Procedures for the Solution of Nonlinear Finite Element Equations." Computer Methods in Applied Mechanics and Engineering, vol. 22, pp. 59–85, 1980.

Bogetti, T. A., J. W. Gillespie, Jr., and M. Lamontia. "Influence of Ply Waviness on Stiffness and Strength Reduction of Composite Laminates." Technical Report CCM-91-27, Center for Composite Materials, University of Delaware, Newark, DE, 1991a.

Bogetti, T. A., J. W. Gillespie, Jr., and M. Lamontia. "Influence of Undulating Cross-Over Regions on Stiffness and Strength Reduction in Composite Laminates." Technical Report CCM-91-29, Center for Composite Materials, University of Delaware, Newark, DE, 1991b.

Chou, P. C., J. Carleone, and C. M. Hsu. "Elastic Constants of Layered Media." Journal of Composite Materials, vol. 6, pp. 80-93, 1972.

Garala, H. J. "Structural Evaluation of 8-Inch Diameter Graphite-Epoxy Composite Cylinders Subjected to External Hydrostatic Compressive Loading." Technical Report, DTRC-89/016, David Taylor Research Center, Bethesda, MD, 1989.

Highsmith, A. L., J. J. Davis, and K. L. E. Helms. "The Influence of Fiber Waviness on the Compressive Behavior of Unidirectional Continuous Fiber Composites." Composites Materials: Testing and Design (Tenth Volume). ASTM STP 1120, edited by Glenn C. Grimes, American Society for Testing and Materials, Philadelphia, PA, pp. 20–36, 1992.

Hyer, M. W., L. C. Maas, and H. P. Fuchs. "The Influence of Layer Waviness on the Stress State in Hydrostatically Loaded Cylinders." Journal of Reinforced Plastics and Composites, vol. 7, no. 11, pp. 601–613, 1988.

Jortner, J. "A Model for Predicting Thermal and Elastic Constants of Wrinkled Regions in Composite Materials." Effects of Defects in Composite Materials, ASTM STP 836, American Society for Testing and Materials, pp. 217–236, 1984.

Lekhnitski, S. G. Theory of Elasticity of an Anisotropic Elastic Body. San Fransisco, CA: Holden-Day, 1963.

Richard, R. M., and J. R. Blackloak. "Finite Element Analysis of Inelastic Structures." AIAA Journal, vol. 7, pp. 432–438, 1969.

Telgadas, H. K., and M. W. Hyer. "The Influence of Layer Waviness of the Stress State in Hydrostatically Loaded Cylinders: Further Results." Journal of Reinforced Plastics and Composites, vol. 9, no. 5, pp. 503–518, 1990.

INTENTIONALLY LEFT BLANK.

No. of Copies	Organization
2	Administrator Defense Technical Info Center ATTN: DTIC-DDA Cameron Station Alexandria, VA 22304-6145
1	Commander U.S. Army Materiel Command ATTN: AMCAM 5001 Eisenhower Ave. Alexandria, VA 22333-0001
1	Director U.S. Army Research Laboratory ATTN: AMSRL-OP-SD-TA, Records Management 2800 Powder Mill Rd. Adelphi, MD 20783-1145
3	Director U.S. Army Research Laboratory ATTN: AMSRL-OP-SD-TL, Technical Library 2800 Powder Mill Rd. Adelphi, MD 20783-1145
1	Director U.S. Army Research Laboratory ATTN: AMSRL-OP-SD-TP, Technical Publishing Branch 2800 Powder Mill Rd. Adelphi, MD 20783-1145
2	Commander U.S. Army Armament Research, Development, and Engineering Center ATTN: SMCAR-TDC Picatinny Arsenal, NJ 07806-5000
1	Director Benet Weapons Laboratory U.S. Army Armament Research, Development, and Engineering Center ATTN: SMCAR-CCB-TL Watervliet, NY 12189-4050
1	Director U.S. Army Advanced Systems Research and Analysis Office (ATCOM) ATTN: AMSAT-R-NR, M/S 219-1 Ames Research Center Moffett Field, CA 94035-1000

No. of Copies	Organization
1	Commander U.S. Army Missile Command ATTN: AMSMI-RD-CS-R (DOC) Redstone Arsenal, AL 35898-5010
1	Commander U.S. Army Tank-Automotive Command ATTN: AMSTA-JSK (Armor Eng. Br.) Warren, MI 48397-5000
1	Director U.S. Army TRADOC Analysis Command ATTN: ATRC-WSR White Sands Missile Range, NM 88002-5502
1	Commandant U.S. Army Infantry School ATTN: ATSH-WCB-O Fort Benning, GA 31905-5000
	Aberdeen Proving Ground
2	Dir, USAMSAA ATTN: AMXSY-D AMXSY-MP, H. Cohen
1	Cdr, USATECOM ATTN: AMSTE-TC
1	Dir, USAERDEC ATTN: SCBRD-RT
1	Cdr, USACBDCOM ATTN: AMSCB-CII
1	Dir, USARL ATTN: AMSRL-SL-I
5	Dir, USARL ATTN: AMSRL-OP-AP-L

No. of Copies	Organization
1	HQDA (SARD-TT/Dr. F. Milton) Washington, DC 20310-0103
1	HQDA (SARD-TT/Mr. J. Appel) Washington, DC 20310-0103
1	Director U.S. Army Research Laboratory ATTN: AMSRL-CP-CA, D. Snider 2800 Powder Mill Road Adelphi, MD 20783
6	Director U.S. Army Research Laboratory ATTN: AMSRL-MA-P, L. Johnson B. Halpin T. Chou AMSRL-MA-PA, D. Granville W. Haskell AMSRL-MA-MA, G. Hagnauer Watertown, MA 02172-0001
4	Commander U.S. Army Armament Research, Development, and Engineering Center ATTN: SMCAR-FSE, T. Gora E. Andricopoulos B. Knutelsky A. Graf Picatinny Arsenal, NJ 07806-5000
3	Commander U.S. Army Armament Research, Development, and Engineering Center ATTN: SMCAR-TD, R. Price V. Linder T. Davidson Picatinny Arsenal, NJ 07806-5000
1	Commander U.S. Army Armament Research and Development Center ATTN: F. McLaughlin Picatinny Arsenal, NJ 07806

No. of Copies	Organization
5	Commander U.S. Army Armament Research, Development, and Engineering Center ATTN: SMCAR-CCH-T, S. Musalli P. Christian K. Fehsal N. Krasnow R. Carr Picatinny Arsenal, NJ 07806-5000
1	Commander U.S. Army Armament Research, Development, and Engineering Center ATTN: SMCAR-CCH-V, E. Fennell Picatinny Arsenal, NJ 07806-5000
1	Commander U.S. Army Armament Research, Development, and Engineering Center ATTN: SMCAR-CCH, J. DeLorenzo Picatinny Arsenal, NJ 07806-5000
2	Commander U.S. Army Armament Research, Development, and Engineering Center ATTN: SMCAR-CC, J. Hedderich Col. Sinclair Picatinny Arsenal, NJ 07806-5000
1	Commander U.S. Army Armament Research, Development, and Engineering Center ATTN: SMCAR-CCH-P, J. Lutz Picatinny Arsenal, NJ 07806-5000
2	Commander U.S. Army Armament Research, Development, and Engineering Center ATTN: SMCAR-FSA-M, D. DeMella F. Diorio Picatinny Arsenal, NJ 07806-5000
1	Commander U.S. Army Armament Research, Development, and Engineering Center SMCAR-FSA, C. Spinelli Picatinny Arsenal, NJ 07806-5000

No. of Copies	Organization
11	Director Benet Laboratories ATTN: SMCAR-CCB, C. Kitchens J. Keane T. Allen J. Vasilakis G. Friar T. Simkins V. Montvori J. Wrzochalski G. D'Andrea R. Hasenbein SMCAR-CCB-R, S. Sopok Watervliet, NY 12189
1	Commander ATTN: SMCWV-QAE-Q, C. Howd Bldg 44 Watervliet Arsenal Watervliet, NY 12189-4050
1	Commander ATTN: SMCWV-SPM, T. McCloskey Bldg 25/3, Watervliet Arsenal Watervliet, NY 12189-4050
1	Commander Watervliet Arsenal ATTN: SMCWV-QA-QS, K. Insco Watervliet, NY 12189-4050
1	Commander Production Base Modernization Activity U.S. Army Armament Research, Development, and Engineering Center ATTN: AMSMC-PBM-K Picatinny Arsenal, NJ 07806-5000
1	Commander U.S. Army Belvoir RD&E Center ATTN: STRBE-JBC, C. Kominos Fort Belvoir, VA 22060-5606
1	U.S. Army Cold Regions Research and Engineering Laboratory ATTN: P. Dutta 72 Lyme Road Hanover, NH 03755

No. of Copies	Organization
1	Director U.S. Army Research Laboratory ATTN: AMSRL-WT-L, D. Woodbury 2800 Powder Mill Road Adelphi, MD 20783-1145
3	Commander U.S. Army Missile Command ATTN: AMSMI-RD, W. McCorkle AMSMI-RD-ST, P. Doyle AMSMI-RD-ST-CN, T. Vandiver Redstone Arsenal, AL 35898
2	U.S. Army Research Office Dir., Math & Computer Sciences Div. ATTN: Andrew Crowson J. Chandra P.O. Box 12211 Research Triangle Park, NC 27709-2211
1	U.S. Army Research Office Engineering Sciences Div ATTN: G. Anderson P.O. Box 12211 Research Triangle Park, NC 27709-2211
2	Project Manager SADARM Picatinny Arsenal, NJ 07806-5000
2	Project Manager Tank Main Armament Systems ATTN: SFAE-AR-TMA, COL Bregard C. Kimker Picatinny Arsenal, NJ 07806-5000
3	Project Manager Tank Main Armament Systems ATTN: SFAE-AR-TMA-MD, H. Yuen J. McGreen R. Kowalski Picatinny Arsenal, NJ 07806-5000

No. of Copies	Organization
2	Project Manager Tank Main Armament Systems ATTN: SFAE-AR-TMA-MS, R. Joinson D. Guziewicz Picatinny Arsenal, NJ 07806-5000
1	Project Manager Tank Main Armament Systems SFAE-AR-TMA-MP, W. Lang Picatinny Arsenal, NJ 07806-5000
2	PEO-Armaments ATTN: SFAE-AR-PM, D. Adams T. McWilliams Picatinny Arsenal, NJ 07806-5000
1	PEO-Field Artillery Systems ATTN: SFAE-FAS-PM, H. Goldman Picatinny Arsenal, NJ 07806
4	Project Manager, AFAS ATTN: LTC D. Ellis G. delCoco J. Shields B. Machak Picatinny Arsenal, NJ 07806-5000
2	Commander DARPA ATTN: J. Kelly B. Wilcox 3701 North Fairfax Drive Arlington, VA 22203-1714
2	Commander Wright-Patterson Air Force Base ATTN: WL/FIV, A. Mayer Dayton, OH 45433
2	NASA Langley Research Center Mail Stop 266 ATTN: AMSRL-VS, W. Elber F. Barlett, Jr. Hampton, VA 23681-0001

No. of Copies	Organization
2	Naval Surface Warfare Center Dahlgren Division Code G33 Dahlgren, VA 224488
1	Naval Research Laboratory Code 6383 ATTN: I. Wolock Washington, DC 20375-5000
1	Office of Naval Research Mech Div Code 1132SM ATTN: Yapa Rajapakse Arlington, VA 22217
1	Naval Ordnance Station Advanced Systems Technology Br. ATTN: D. Holmes Code 2011 Louisville, KY 40214-5245
1	David Taylor Research Center Ship Structures and Protection Department ATTN: J. Corrado, Code 1702 Bethesda, MD 20084
2	David Taylor Research Center ATTN: R. Rockwell W. Phyillaier Bethesda, MD 20054-5000
5	Director Lawrence Livermore National Laboratory ATTN: R. Christensen S. deTeresa W. Feng F. Magness M. Finger P.O. Box 808 Livermore, CA 94550
1	Director Los Alamos National Laboratory ATTN: D. Rabern MEE-13, Mail Stop J-576 P.O. Box 1633 Los Alamos, NM 87545

No. of Copies	Organization
1	Oak Ridge National Laboratory ATTN: R. M. Davis P.O. Box 2008 Oak Ridge, TN 37831-6195
1	Battelle PNL ATTN: M. Smith P.O. Box 999 Richland, WA 99352
6	Director Sandia National Laboratories Applied Mechanics Department, Division-8241 ATTN: C. Robinson G. Benedetti W. Kawahara K. Perano D. Dawson P. Nielan P.O. Box 969 Livermore, CA 94550-0096
1	Drexel University ATTN: Albert S.D. Wang 32nd and Chestnut Streets Philadelphia, PA 19104
2	North Carolina State University Civil Engineering Department ATTN: W. Rasdorf L. Spainhour P.O. Box 7908 Raleigh, NC 27696-7908
1	Pennsylvania State University ATTN: David W. Jensen 223-N Hammond University Park, PA 16802
1	Pennsylvania State University ATTN: Richard McNitt 227 Hammond Bldg University Park, PA 16802
1	Pennsylvania State University ATTN: Renata S. Engel 245 Hammond Building University Park, PA 16801

No. of Copies	Organization
1	Purdue University School of Aero & Astro ATTN: C.T. Sun W. Lafayette, IN 47907-1282
1	Stanford University Department of Aeronautics and Aeroballisticss Durant Building ATTN: S. Tsai Stanford, CA 94305
1	UCLA MANE Dept, Engrg IV ATTN: H. Thomas Hahn Los Angeles, CA 90024-1597
2	Univ of Dayton Research Inst ATTN: Ran Y. Kim Ajit K. Roy 300 College Park Avenue Dayton, OH 45469-0168
1	University of Dayton ATTN: James M. Whitney 300 College Park Ave Dayton, OH 45469-0240
2	University of Delaware Center for Composite Materials ATTN: J. Gillespe M. Santare 201 Spencer Laboratory Newark, DE 19716
1	University of Illinois at Urbana-Champaign National Center for Composite Materials Research 216 Talbot Laboratory ATTN: J. Economy 104 South Wright Street Urbana, IL 61801
1	University of Kentucky ATTN: Lynn Penn 763 Anderson Hall Lexington, KY 40506-0046

No. of Copies	Organization
1	The University of Texas at Austin Center for Electromechanics ATTN: J. Price 10100 Burnet Road Austin, TX 78758-4497
1	University of Utah Department of Mechanical and Industrial Engineering ATTN: S. Swanson Salt Lake City, UT 84112
2	Virginia Polytechnical Institute & State University Dept of ESM ATTN: Michael W. Hyer Kenneth L. Reifsnider Blacksburg, VA 24061-0219
1	ARMTEC Defense Products ATTN: Steve Dyer 85-901 Avenue 53 P.O. Box 848 Coachella, CA 92236
2	Advanced Composite Materials Corporation ATTN: P. Hood J. Rhodes 1525 S. Buncombe Road Greer, SC 29651-9208
1	Alliant Techsystems, Inc. ATTN: J. Bode C. Candland L. Osgood R. Buretta R. Becker M. Swenson 600 Second St. NE Hopkins, MN 55343
1	Amoco Performance Products, Inc. ATTN: M. Michno, Jr. 4500 McGinnis Ferry Road Alpharetta, GA 30202-3944

No. of Copies	Organization
1	Applied Composites ATTN: W. Grisch 333 North Sixth Street St. Charles, IL 60174
1	Brunswick Defense ATTN: T. Harris Suite 410 1745 Jefferson Davis Hwy. Arlington, VA 22202
1	Chamberlain Manufacturing Corporation Research and Development Division ATTN: T. Lynch P.O. Box 2335 550 Esther Street Waterloo, IA 50704
1	Chamberlain Manufacturing Corporation Research and Development Division ATTN: M. Townsend P.O. Box 2545 550 Esther Street Waterloo, IA 50704
1	Custom Analytical Engineering Systems, Inc. ATTN: A. Alexander Star Route, Box 4A Flintstone, MD 21530
1	General Dynamics Land Systems Division ATTN: D. Bartle P.O. Box 1901 Warren, MI 48090
3	Hercules, Incorporated ATTN: R. Boe F. Policelli J. Poesch P.O. Box 98 Magna, UT 84044

No. of Copies	Organization
3	Hercules, Incorporated ATTN: G. Kuebeler J. Vermeychuk B. Manderville, Jr. Hercules Plaza Wilmington, DE 19894
1	Hexcel ATTN: M. Shelendich 11555 Dublin Blvd. P.O. Box 2312 Dublin, CA 94568-0705
1	IAP Research, Inc. ATTN: A. Challita 2763 Culver Avenue Dayton, Ohio 45429
2	Institute for Advanced Technology ATTN: T. Kiehne H. Fair P. Sullivan 4030-2 W. Braker Lane Austin, TX 78759
1	Integrated Composite Technologies ATTN: H. Perkinson, Jr. P.O. Box 397 York New Salem, PA 17371-0397
1	Interferometrics, Inc. ATTN: R. Larriva, Vice President 8150 Leesburg Pike Vienna, VA 22100
2	Kaman Sciences Corporation ATTN: D. Elder T. Hayden P.O. Box 7463 Colorado Springs, CO 80933
3	LORAL/Vought Systems ATTN: G. Jackson K. Cook L.L. Hadden 1701 West Marshall Drive Grand Prairie, TX 75051

No. of Copies	Organization
2	Martin-Marietta Corp. ATTN: P. Dewar L. Sponar 230 East Goddard Blvd. King of Prussia, PA 19406
2	Olin Corporation Flinchbaugh Division ATTN: E. Steiner B. Stewart P.O. Box 127 Red Lion, PA 17356
1	Olin Corporation ATTN: L. Whitmore 10101 9th St., North St. Petersburg, FL 33702
1	Rennsaeler Polytechnic Institute ATTN: R. B. Pipes Troy, NY 12180
1	SPARTA, Inc. ATTN: J. Glatz 9455 Towne Centre Drive San Diego, CA 92121-1964
2	United Defense LP ATTN: P. Para G. Thomas 1107 Coleman Avenue, Box 367 San Jose, CA 95103

No. of Copies	Organization
	Aberdeen Proving Ground
64	Dir, USARL
	ATTN: AMSRL-CI,
	C. Mermegan (394)
	AMSRL-CI-C,
	W. Sturek (1121)
	AMSRL-CI-CB,
	R. Kaste (394)
	AMSRL-CI-S,
	A. Mark (309)
	AMSRL-SL-B,
	P. Dietz (328)
	AMSRL-SL-BA,
	J. Walbert (1065)
	AMSRL-SL-BL,
	D. Bely (328)
	AMSRL-SL-I,
	D. Haskill (1065)
	AMSRL-WT-P,
	A. Horst (390A)
	AMSRL-WT-PA,
	T. Minor (390)
	C. Leveritt (390)
	D. Kooker (390A)
	AMSRL-WT-PB,
	E. Schmidt (120)
	P. Plostins (120)
	AMSRL-WT-PC,
	R. Fifer (390A)
	AMSRL-WT-PD,
	B. Burns (390)
	W. Drysdale (390)
	K. Bannister (390)
	T. Bogetti (390)
	J. Bender (390)
	R. Murray (390)
	R. Kirkendall (390)
	T. Erline (390)
	D. Hopkins (390)
	S. Wilkerson (390)
	C. McCall (390)
	D. Henry (390)
	R. Kaste (390)
	L. Burton (390)
	J. Tzeng (390)
	R. Lieb (390)
	G. Gazonas (390)
	M. Leadore (390)
	C. Hoppel (390)

No. of Copies	Organization
	AMSRL-WT-PD(ALC)
	A. Abrahamian
	K. Barnes
	M. Berman
	H. Davison
	A. Frydman
	T. Li
	W. McIntosh
	E. Szymanski
	AMSRL-WT-T,
	W. Morrison (309)
	AMSRL-WT-TA,
	W. Gillich (390)
	W. Bruchey (390)
	AMSRL-WT-TC,
	K. Kimsey (309)
	R. Coates (309)
	W. de Rosset (309)
	AMSRL-WT-TD,
	D. Dietrich (309)
	G. Randers-Pehrson (309)
	J. Huffington (309)
	A. Das Gupta (309)
	J. Santiago (309)
	AMSRL-WT-W,
	C. Murphy (120)
	AMSRL-WT-WA,
	H. Rogers (394)
	B. Moore (394)
	A. Baran (394)
	AMSRL-WT-WB,
	F. Brandon (120)
	W. D'Amico (120)
	AMSRL-WT-WC,
	J. Rocchio (120)
	AMSRL-WT-WD,
	A. Zielinski (120)
	J. Powell (120)
	AMSRL-WT-WE,
	J. Temperley (120)
	J. Thomas (394)

USER EVALUATION SHEET/CHANGE OF ADDRESS

This Laboratory undertakes a continuing effort to improve the quality of the reports it publishes. Your comments/answers to the items/questions below will aid us in our efforts.

1. ARL Report Number ARL-TR-585 Date of Report October 1994

2. Date Report Received _____

3. Does this report satisfy a need? (Comment on purpose, related project, or other area of interest for which the report will be used.) _____

4. Specifically, how is the report being used? (Information source, design data, procedure, source of ideas, etc.) _____

5. Has the information in this report led to any quantitative savings as far as man-hours or dollars saved, operating costs avoided, or efficiencies achieved, etc? If so, please elaborate. _____

6. General Comments. What do you think should be changed to improve future reports? (Indicate changes to organization, technical content, format, etc.) _____

CURRENT ADDRESS

_____
Organization

_____
Name

_____
Street or P.O. Box No.

_____
City, State, Zip Code

7. If indicating a Change of Address or Address Correction, please provide the Current or Correct address above and the Old or Incorrect address below.

OLD ADDRESS

_____
Organization

_____
Name

_____
Street or P.O. Box No.

_____
City, State, Zip Code

(Remove this sheet, fold as indicated, tape closed, and mail.)
(DO NOT STAPLE)

DEPARTMENT OF THE ARMY

OFFICIAL BUSINESS

NO POSTAGE
NECESSARY
IF MAILED
IN THE
UNITED STATES

BUSINESS REPLY MAIL
FIRST CLASS PERMIT NO 0001, APG, MD

Postage will be paid by addressee

Director
U.S. Army Research Laboratory
ATTN: AMSRL-OP-AP-L
Aberdeen Proving Ground, MD 21005-5066